Materials Science and Engineering A 528 (2011) 5066–5072

Contents lists available at ScienceDirect

Materials Science and Engineering A

journal homepage: www.elsevier.com/locate/msea

Development of a novel severe plastic deformation method for tubular materials: Tube Channel Pressing (TCP)

A. Zangiabadi, M. Kazeminezhad *

Department of Materials Science and Engineering, Sharif University of Technology, Azadi Avenue, Tehran, Iran

ARTICLE INFO

Article history:
Received 8 December 2010
Received in revised form 20 February 2011
Accepted 2 March 2011
Available online 9 March 2011

Keywords:
Tube Channel Pressing (TCP)
Severe plastic deformation (SPD)
Aluminum tube
Mechanical properties
Microstructure

ABSTRACT

A new severe plastic deformation (SPD) method entitled Tube Channel Pressing (TCP) is proposed. In this study, the ability of TCP on strength improvement and grain refinement is assessed. This method is based on pressing a tube through a tubular channel die with a neck zone. Utilization of a mandrel fitted inside the tube prevents the crumpling of tube and preserves its initial dimension. Due to the symmetric design, after one pass, the die is rotated upside down and the second pass is applied by pressing the tube in inverse direction. Ultimate strength of a commercial purity aluminum tube after 5 successful passes is improved to 2 times of the initial strength. Analytical calculations and simulation of this process accompanied by commercial finite element code ABAQUS/Explicit demonstrate that the total average equivalent strain of 1.2 is imposed in each pass. Furthermore, hardness distribution through tube thickness is assessed. Then, ability of TCP in grain refinement of tubular samples after each pass is determined.

1. Introduction

In 20 recent years, producing ultrafine-grained (UFG) materials due to their superior physical and mechanical properties has attracted a great deal of attention. Many methods have been introduced for producing these materials in bulk forms of rods, sheets and disks, without any contamination or porosity; named severe plastic deformation (SPD) [1]. Some of the most successful SPD processes for producing UFG rods are equal channel angular pressing (ECAP) [2,3], cyclic extrusion compression (CEC) [4]; accumulative roll bonding (ARB) for sheets [5]; and high pressure torsion (HPT) for disks [6]. Nevertheless, economic feasibility, low productivity rate, fabricating convenience and eventually confined industrialization of these materials are still of a big concern [7]. Moreover, limited works have been carried out on development of tubular UFG materials, such as high pressure tube twisting (HPTT) [8] and Accumulative Spin-Bonding (ASB) [9]. However, tubes are the most practical essentials in aerospace, automobile, building construction, petroleum industries, etc. Therefore, it is sensible to pay further attention for these sorts of UFG materials.

In this study, a new SPD process has been introduced for tubes; named Tube Channel Pressing (TCP) and shown schematically in Fig. 1(a). Comparing this process with the HPTT method, some advantages can be mentioned: (1) More homogeneous strain can be imposed to tube through TCP, (2) the tools for TCP are simple and thus it requires low cost, (3) the longer tubes can be produced through TCP. Moreover, the advantage of TCP over ASB is that in ASB it may be possible to find imperfect bond between layers.

2. Principle of TCP

The principle of TCP deformation is based on pressing a tube through the channel which has a neck zone shown in Fig. 1. A mandrel is utilized to make a tubular channel and prevents the crumpling of tube. In this manner, through passing the tube from neck zone, the thickness of tube remains constant. After applying one pass, the ram is pulled out and the whole die is rotated 180° vertically, and the second pass is applied in the same manner (Fig. 1(b) and (c)).

3. Strain analysis

Illustration of tubular channel in Fig. 2 can be useful in order to analyse the applied strain in each pass. In this regard, deformation zone (neck zone) is separated to 3 regions with a similar radius of curvature; named: (i), (ii) and (iii) (Fig. 2(b)). Each of these symmetric regions resembles the ECAP die introduced by Luis Pérez (Fig. 3) [10]. This ECAP die has some similarities with the regions in TCP die: (1) the same inner and outer radii in the deformation zone, (2) the constancy of channel section throughout the die. However, there is a disparity between axisymmetric configuration of TCP and 2-dimensional layout of ECAP which necessitates additional consideration.

* Corresponding author. Tel.: +98 21 66165227; fax: +98 21 66005717.
E-mail address: mkazemi@sharif.edu (M. Kazeminezhad).

0921-5093/$ – see front matter © 2011 Elsevier B.V. All rights reserved.
doi:10.1016/j.msea.2011.03.012

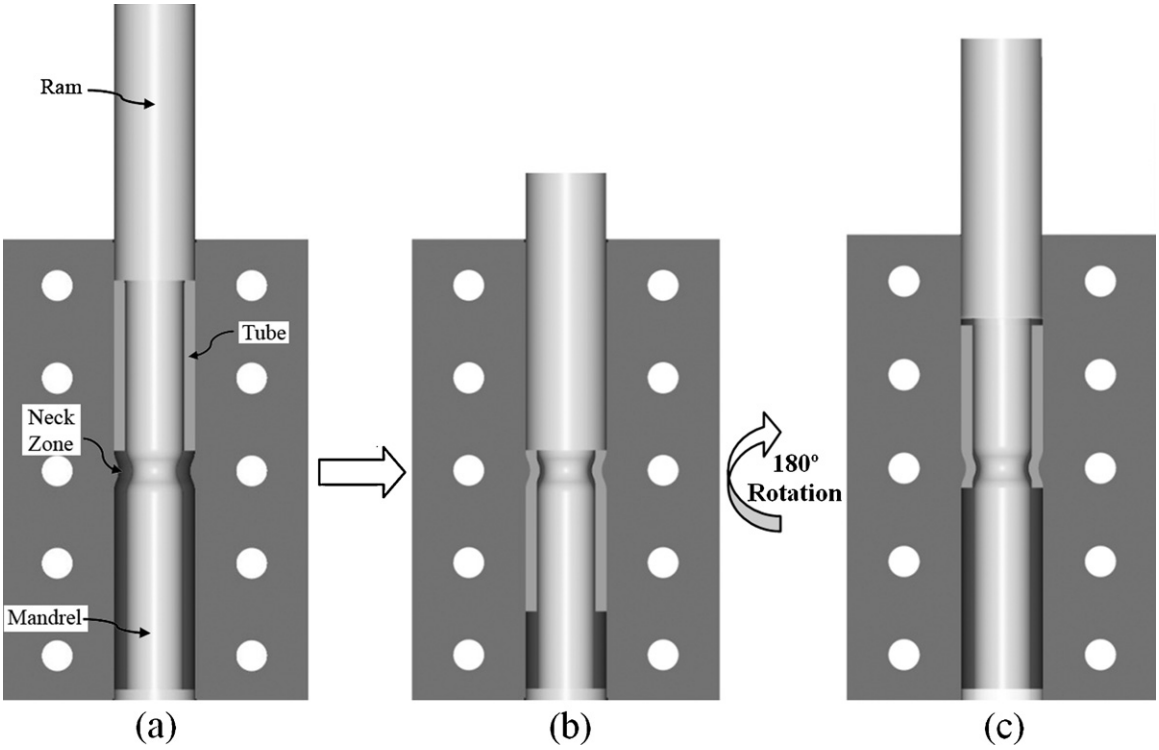

Fig. 1. Schematic and procedure of TCP; (a) beginning of the first pass, (b) the end of the first pass and (c) beginning of the second pass.

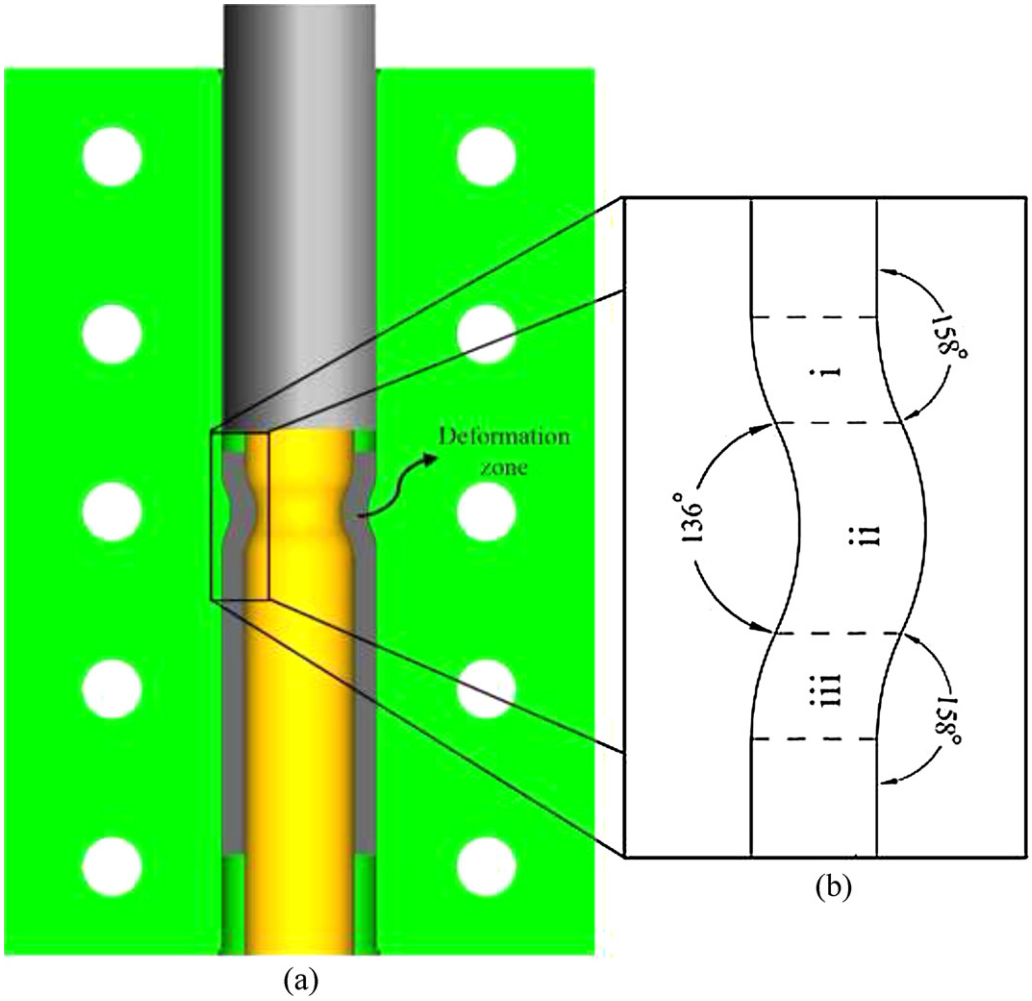

Fig. 2. Schematic of (a) TCP die and (b) deformation zone in channel (three curvatures named i, ii, iii).

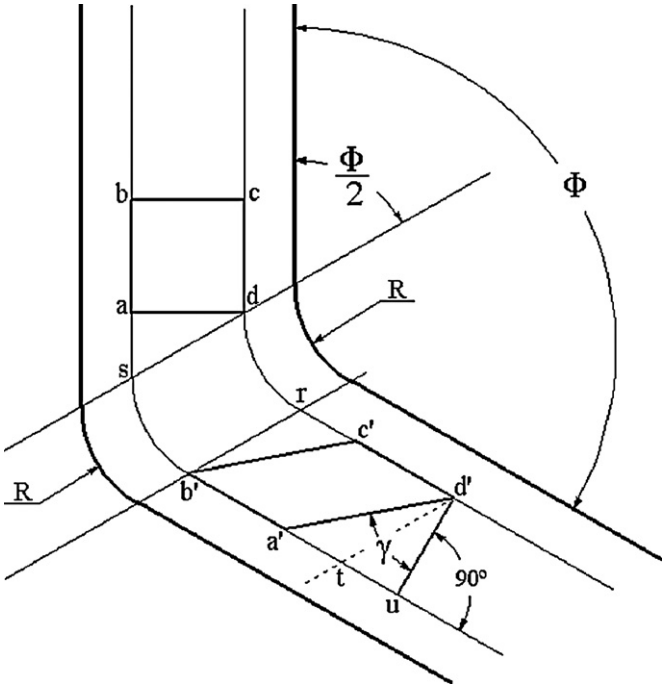

Fig. 3. ECAP die with equal fillet radius introduced by Luis Pérez [10].

According to the Misses criterion, Eq. (1) [10] calculates the equivalent strain in the ECAP die with equal fillet radius (Fig. 3), and also it is capable of roughly calculation of equivalent strain for each region of TCP die:

$$\bar{\varepsilon}_{\text{von-Mises}} = \frac{2}{\sqrt{3}} \cot\left(\frac{\Phi}{2}\right) \tag{1}$$

where, Φ is the angle of shearing in each curvature. The angle of curvatures (i) and (iii) is 158°, and that of curvature (ii) is 136° (Fig. 2(b)). So, the equivalent strain in TCP die after one pass is, 0.224 (for curvature (i)) +0.470 (for curvature (ii)) +0.224 (for curvature (iii)) ≅ 0.92. Moreover, the tube cross section area is constant through passing the neck zone. Since after decreasing tube diameter, it is deformd back to the initial dimension, the related homogenous strain must be doubled. Hence, the homogenous strain can be calculated as follows [11]:

$$\bar{\varepsilon}_{\text{Hom}} = \frac{4}{\sqrt{3}} \ln\left(\frac{D_m}{d_m}\right) \tag{2}$$

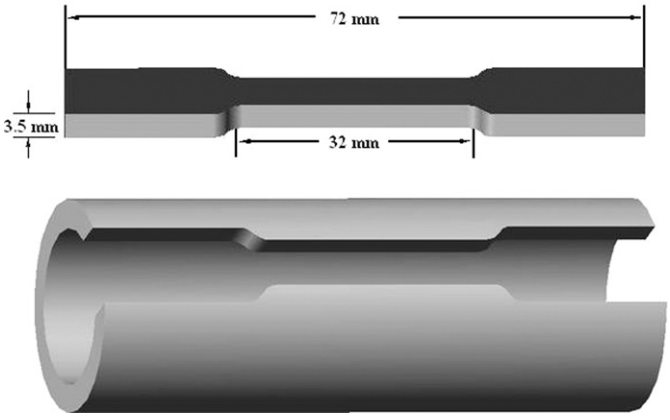

Fig. 5. Tensile sample from the tube.

where, D_m is the average diameter of inner and outer sides of the channel and d_m is the average diameter of the inner and outer sides of the neck zone, i.e. 22.5 mm 19.5 mm, respectively. Therefore, total effective strain achieved after one pass is:

$$\bar{\varepsilon}_{\text{eff.}} \simeq \bar{\varepsilon}_{\text{von-Mises}} + \bar{\varepsilon}_{\text{Hom.}} = 0.92 + 0.33 = 1.25 \tag{3}$$

TCP exerts appreciable strain, however for authenticity; this value is analogized with the value obtained from finite element code ABAQUS/Explicit simulation. The simulation is based on symmetrical model which has identical geometrical and mechanical properties as those for experimental operations. In this regard, the approximate strain that accumulated at the middle of tube thickness is calculated 1.2 (Fig. 4), which is consistent with the value achieved from analytical calculation. Moreover, from the magnified region and configuration of the elements, it can be concluded that the deformation mainly occurs in shear mode.

4. Experimental procedures

Tube of 26 mm outer and 19 mm inner diameters was selected from commercial purity aluminum (AA1050) and cut into 70 mm long pieces and then annealed at 623 K for 3 h.

Surfaces of aluminum samples and internal die surfaces were sprayed with MoS_2 lubricant. The die was stood vertically and the sample was inserted by a ram into the channel (Fig. 1(a)). TCP was carried out with a 1000 kN hydraulic pressing machine at a ram speed of 0.5 mm/s at room temperature. The applied load in this process was in range of 40–80 kN.

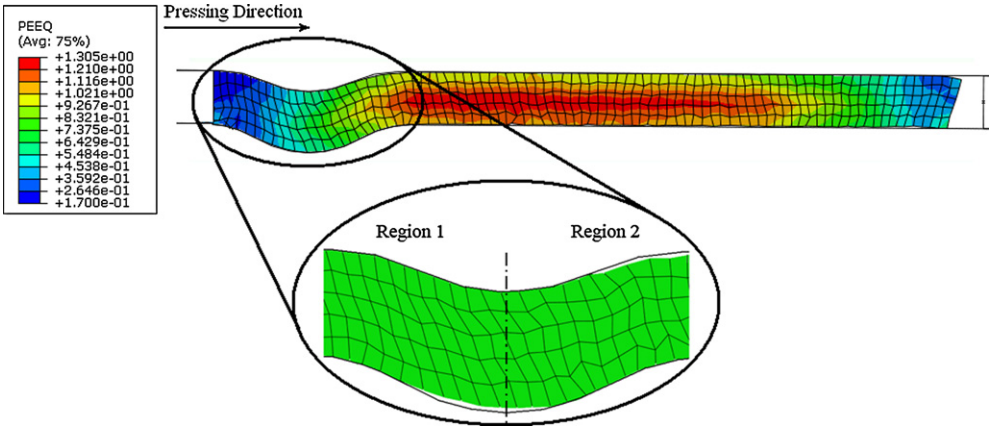

Fig. 4. ABAQUS simulation; strain distribution after 1 TCP pass in the longitudinal section of a tube.

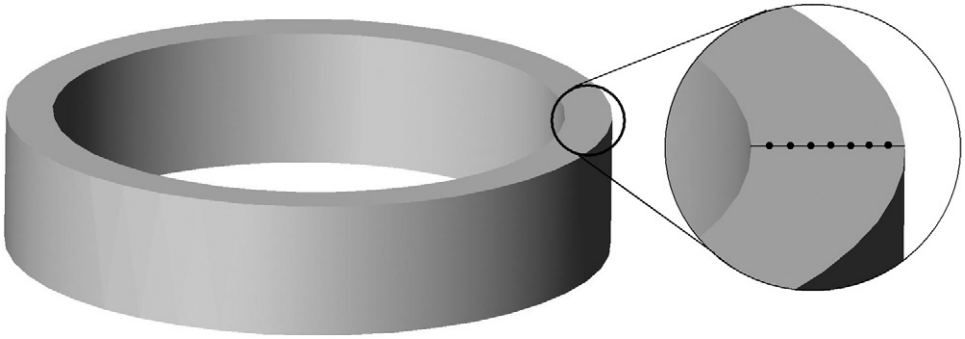

Fig. 6. Locations for measuring Vickers micro hardness.

In order to study the mechanical properties of the aluminum tubes after TCP, tensile and hardness tests were carried out. Tensile samples were cut out from longitudinal direction of the tube according to the ASTM E8M (Fig. 5).

Vickers hardness test was carried out on the cross section of the tube. The average hardness value of each sample was achieved from 10 different points on the cross section area. Also, to investigate the variation of hardness across the thickness of the tubes after TCP, Vickers micro harness test was carried out on 7 equidistant points in radius direction on the cross section (Fig. 6).

To investigate the microstructure evolution achieved from TCPed tube, X-ray diffraction (XRD) peak profile analysis was conducted on a Philips X-ray diffractometer using Cu Kα radiation that equipped with a graphite monochromator. The X-ray patterns of samples were obtained in the range of 10–80° and in the step width of 0.02°. For calibration of the instrumental line broadening, SiC powder was examined in the same condition. Resolving full-width at half-maximum (FWHM) for all peaks was carried out using the software configured with the XRD system. The XRD patterns were achieved from center of the 15 mm × 10 mm × 1 mm samples, cut from longitudinal direction of TCPed tubes. The analysed area was located 1.5 mm deep from outside wall of the tube (Fig. 7).

An approved reliable based-model approach of X-ray diffraction line profile analysis that utilized in this study is Williamson–Hall method [12]. Correspondingly, crystalline size and lattice equivalent strain can be resolved by measuring the deviation of line profile from perfect crystal diffraction. In the Williamson–Hall method, there is a relation between FWHM (β), crystallite size (t), and the distortion function ($f(\varepsilon)$) (explained in Refs. [12,13]), by the following equation [13]:

$$\beta \cos\theta = \frac{\kappa\lambda}{t} f(\varepsilon) \sin\theta \tag{4}$$

where θ is the Bragg angle, is the wavelength and λ is the Scherer constant. Considering Eq. (4), the intercept of the plot $\beta \cos\theta$ versus $\sin\theta$ gives the cell size and the slope gives the crystal strain.

Commercial diffractometer contains the instrumental profile besides the intrinsic profile (pure diffraction profile). In this regard the Gaussian–Gaussian function can be employed to correct the integral breadths of intrinsic profile [12]:

$$\beta_{\text{exp}}^2 \cong \beta^2 + \beta_{\text{ins}}^2 \tag{5}$$

where β, β_{exp} and β_{ins} are the integral breadth of the intrinsic, experimental and instrumental profile, respectively. The XRD pattern of the 5 TCPed sample can be seen in Fig. 8. Four intense diffraction peaks related to the crystalline planes of (1 1 1), (2 0 0), (2 2 0) and (3 1 1) in all samples are noticeable. Consequently, in this study these four peaks of crystalline planes are considered for grain size calculations.

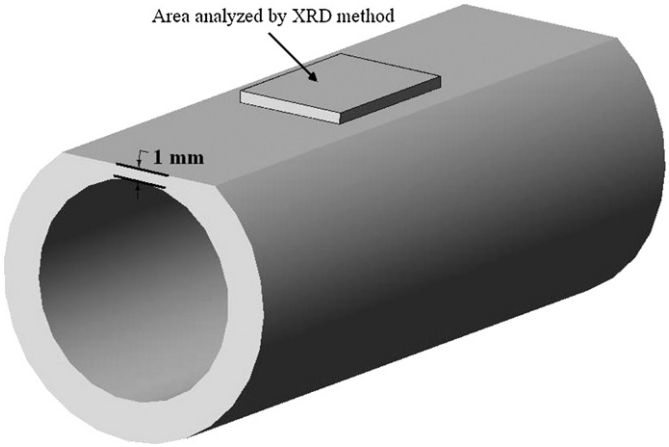

Fig. 7. Schematic of prepared sample for XRD analysis.

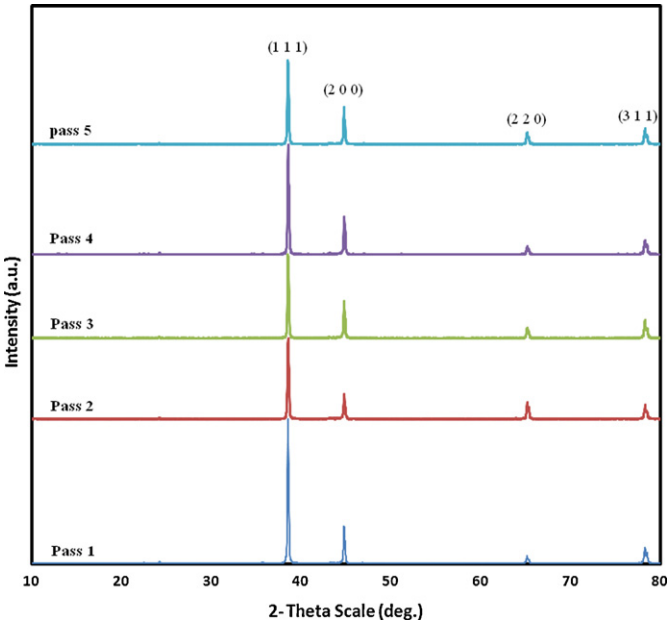

Fig. 8. XRD patterns for TCPed Al tubes.

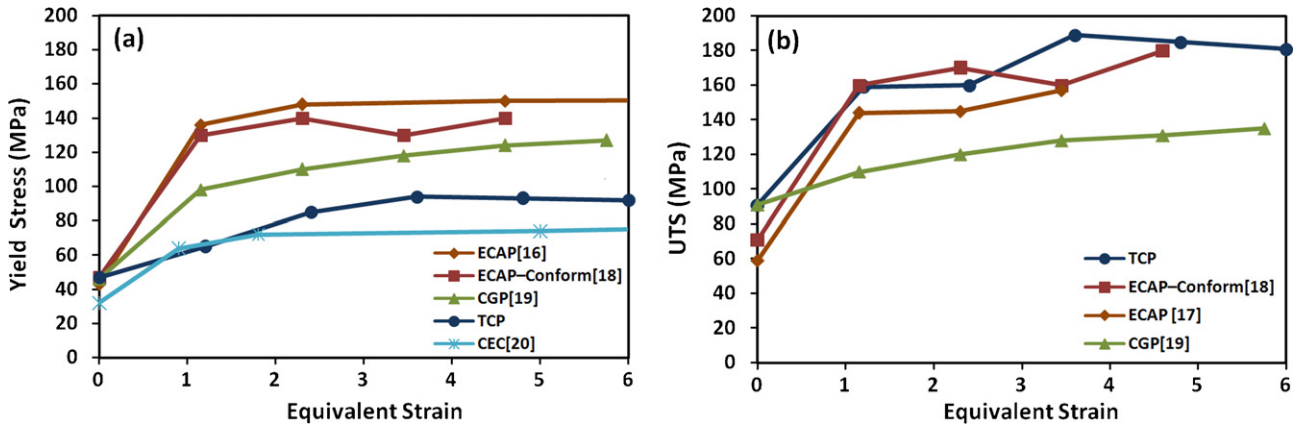

Fig. 9. The effect of strain on the (a) yield stress and (b) UTS through TCP and other SPD methods.

5. Results and discussion

5.1. Mechanical properties

The results of tensile tests after 1–5 successful TCP passes that carried out without any rupture or cracks on the tube are shown in Fig. 9(a) and (b). As can be seen in Fig. 9(a), yield stress of an annealed sample is increased from 47 MPa to 92 MPa after 5 TCP passes, and ultimate tensile stress (UTS) reaches from 91 MPa to over than 185 MPa (Fig. 9(b)). Slight decrease in the yield and UTS values in final passes may be related to flow-softening or micro-cracks through SPD [14,15]. However, the strength variation reveals the effectiveness of TCP for strengthening the Al tubes.

Moreover, Fig. 9(a) and (b) shows tensile test results of some other SPD processes such as ECAP [16,17], ECAP-Conform [18], constrained groove pressing (CGP) [19] and CEC [20]. Comparing these results with those achieved from TCP reveals the reliability of the presented method in strength improvement of tubular materials.

Fig. 10 demonstrates the values of uniform and fracture elongation and the relationship between those. As shown in this figure, both of these elongations after TCP are decreased, however, they remain constant and are slightly increased after second pass. Similar trends have been observed in number of metals such as Al, Cu and some aluminum alloys through SPD [2]. It is proposed that this phenomenon originates from grain boundary sliding and grain rotation mechanisms during deformation [21]. Furthermore, Fig. 10 reveals that the ratio of non-uniform elongation to uniform elongation is increased with increasing the pass number. In other word, the main tensile strains are achieved in the state of plastic instability. This phenomenon, reported earlier, may have its origin in the tendency of superplasticity of SPDed materials [19].

5.2. Hardness

The results of Vickers hardness of samples that obtained from the tubes in annealed condition and after TCP are shown in Fig. 11. Furthermore, the hardness values of commercial purity aluminum samples processed by other SPD processes, such as ECAP [16], CGP [19], CEC [20] and HPT [22] are compared with those of TCPed specimens.

In a general manner, increasing trends of yield stress, UTS and hardness are sharp in initial passes and then get a lower rate in final passes. The strength and hardness of tubes through TCP can be increased up to 2 times of those for annealed tube. These results are consistent with those of other SPD processes.

The results of micro hardness within the thickness of the tube are shown in Fig. 12. The arched trends of the Vickers micro hardness in this figure represent the moderate inhomogeneity of hardness with higher value at mid thickness and lower values at the inner and outer sides of a tube wall. Inner side of the tube has higher hardness value than that in outer side (Fig. 12). It should be noted that the variations of hardness value within the thickness is consistent with the calculated strain variations shown in Fig. 4. Also, a similar result has been reported in ECAP [23]. Moreover, the

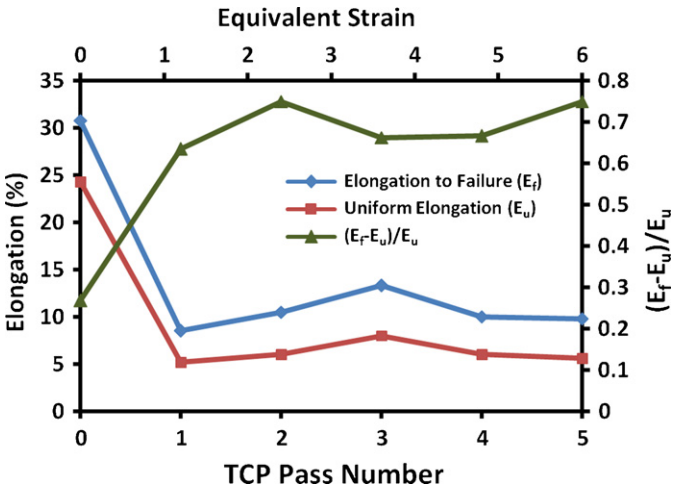

Fig. 10. The effect of strain on the elongation through TCP.

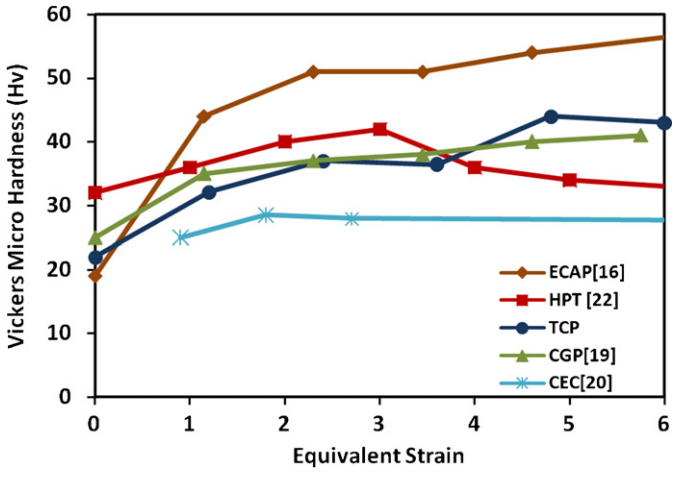

Fig. 11. Macro hardness data for commercial purity Al after processing by TCP and other SPD methods.

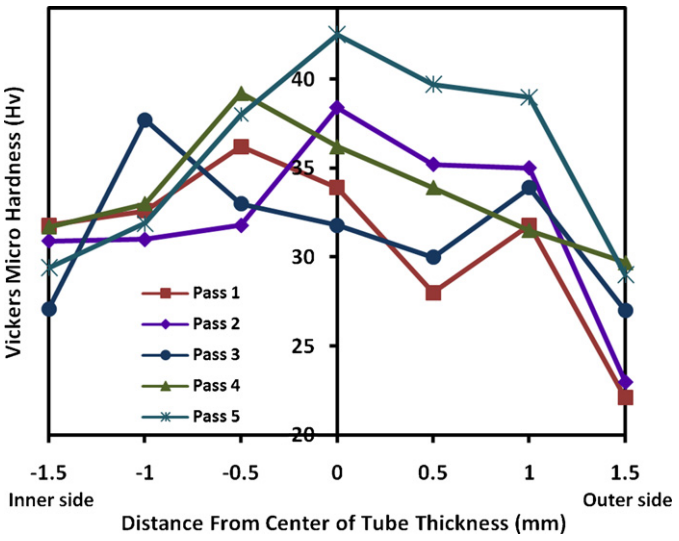

Fig. 12. Micro hardness along tube thickness in each pass.

moderate variation of hardness in thickness shows an advantage with respect to that of HPTT.

5.3. Stereo microscopy

Longitudinal samples cut from the tubes were polished to reach 1 mm deep in thickness. Then, they were etched with modified Poulton's reagent solution [24]. Finally, they were investigated by stereo microscopy accompanied by two-illuminations. The stereo microscopy of annealed sample shows extremely large average grain size, approximately 1000 μm (Fig. 13(a)). After 3 TCP passes the average grain size of Al tube is nearly reduced to 400 μm (Fig. 13(b)), and after 5 TCP passes it reaches to less than 200 μm (Fig. 13(c)). As shown in these figures, deformed microstructures of TCPed samples preserve their initial equiaxed grain structures. This is due to the two opposing shear modes of deformation in the neck zone (Fig. 4) which explained earlier. These two opposing shear modes of deformation, accompanied with the homogenous mode of deformation, lead to grain refinement without any significant change on the grains shape.

5.4. XRD analysis

X-ray diffraction peak profile analysis provides an effective tool for the investigation of microstructures in the bulk materials [25]. For instance, X-ray diffraction method is capable of assessing the crystallite size generally smaller than about 500 nm [26]. During severe plastic deformation, subgrain boundaries evolve in the grains structures [22]. Subsequently, these boundaries develop areas with coherent crystalline domain size [27].

After analysing the XRD pattern of each sample using Williamson–Hall method, the crystallite size in each pass is determined and shown in Fig. 14. As can be seen, after 5 TCP passes the crystallite size of ~360 nm can be achieved. However, the coherent crystalline domain size determined by XRD may be affected by the distribution of dislocations. But, in this case, the

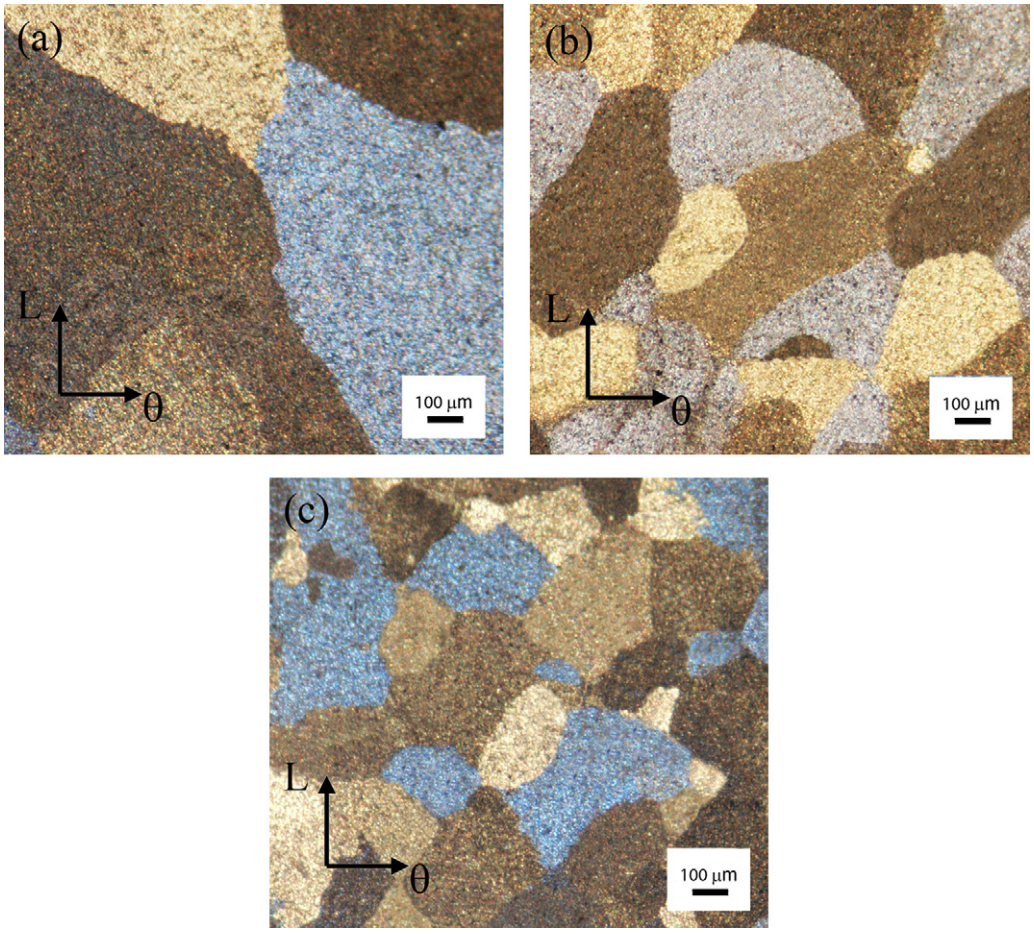

Fig. 13. Metallographic images of (a) an annealed Al tube, (b) a TCPed Al tube after 3 passes and (c) a TCPed Al tube after 5 passes (*L*: longitudinal).

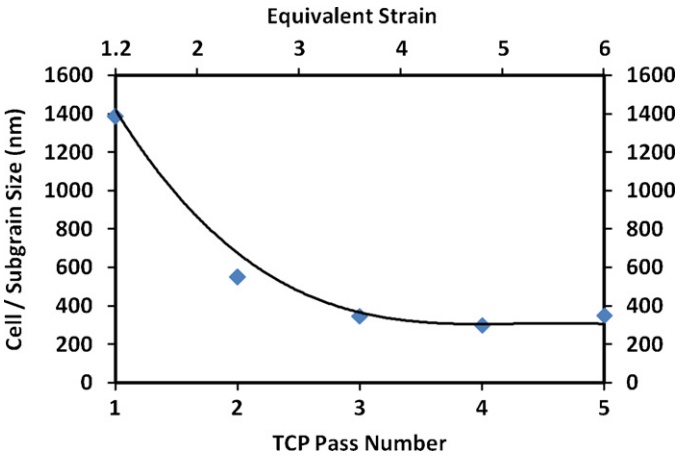

Fig. 14. The cell/subgrain size versus pass number.

crystallite sizes obtained from passes 2 to 5 reach to a same values of cells/subgrains sizes achieved from transmission electron microscopy (TEM) micrographs of ECAP [28,29], CGP [19,30], ARB [5,31]. This proves the ability of TCP in grain refinement.

6. Conclusions

The conclusions from this study can be summarized to:

1. Applying the SPD process on tube is successfully possible, and TCP can be classified as a new SPD method.
2. TCP is successfully carried out in 5 passes without any rupture or cracks, and the yield stress, UTS and hardness are increased up to 2 times of those for the annealed tube.
3. The accumulation of strains in a TCPed sample is the result of mainly shear deformations, and according to the calculations, strain has a considerable value of ~1.2 in each pass.
4. After TCP, the hardness distribution through tube thickness has a maximum at mid thickness and two minimum at inner and outer sides of a tube wall.
5. As a result of applying 5 TCP passes, the average cell size of commercial purity aluminum is decreased to 360 nm.
6. Comparing the results achieved from TCP with those of other SPD processes proves that TCP has a reasonable ability in strength improvement and grain refinement.

Acknowledgement

It is authors' pleasure to express their gratitude to the research board of Sharif University of Technology for the financial support and the provision of the research facilities used in this work.

References

[1] N. Pardis, R. Ebrahimi, Mater. Sci. Eng. A 527 (2009) 355–360.
[2] R.Z. Valiev, T.G. Langdon, Prog. Mater. Sci. 51 (2006) 881–981.
[3] V.M. Segal, Mater. Sci. Eng. A 197 (1995) 157–164.
[4] J. Richert, M. Richert, M. Mroczkowski, Int. J. Mater. 1 (1998) 479–482.
[5] Y. Saito, N. Tsuji, H. Utsunomiya, T. Sakai, R.G. Hong, Scr. Mater. 39 (1998) 1221–1227.
[6] A.P. Zhilyaev, T.G. Langdon, Prog. Mater. Sci. 53 (2008) 893–979.
[7] M. Eizadjou, H. Manesh Danesh, K. Janghorban, J. Alloys Compd. 474 (2009) 406–415.
[8] L.S. Toth, M. Arzaghi, J.J. Fundenberger, B. Beausir, O. Bouaziz, R. Arruffat-massion, Scr. Mater. 60 (2009) 175–177.
[9] M.S. Mohebbi, A. Akbarzadeh, Mater. Sci. Eng. A 528 (2010) 180–188.
[10] C.J. Luis perez, Scr. Mater. 50 (2004) 387–393.
[11] W.F. Hosford, R.M. Caddell, Metal Forming (Mechanics and Metallurgy), 2nd ed., Prentice Hall, Englewood Cliffs, 1993.
[12] Z. Zhang, F. Zhou, E.J. Lavernia, Metall. Mater. Trans. A 34A (2003) 1349–1355.
[13] P. Mukherjee, A. Sarkar, P. Barat, S.K. Bandyopadhyay, P. Sen, S.K. Chattopadhyay, P. Chatterjee, S.K. Chatterjee, M.K. Mitra, Acta Mater. 52 (2004) 5687–5696.
[14] A. Krishnaiah, U. Chakkingal, P. Venugopal, Mater. Sci. Eng. A 410–411 (2005) 337–340.
[15] D.H. Shin, J.-J. Park, Y.-S. Kim, K.-T. Park, Mater. Sci. Eng. A 328 (2002) 98–103.
[16] E.A. El-danaf, M.S. Soliman, A.A. Almajid, M.M. El-rayes, Mater. Sci. Eng. A 458 (2007) 226–234.
[17] A. Sivaraman, U. Chakkingal, J. Mater. Process. Technol. 202 (2008) 543–548.
[18] G.J. Raab, R.Z. Valiev, T.C. Lowe, Y.T. Zhu, Mater. Sci. Eng. A 382 (2004) 30–34.
[19] E. Hosseini, M. Kazeminezhad, Mater. Sci. Eng. A 526 (2009) 219–224.
[20] M. Richert, Q. Liu, N. Hansen, Mater. Sci. Eng. A 260 (1999) 275–283.
[21] R.Z. Valiev, Nat. Mater. 3 (2004) 511–516.
[22] Y. Ito, Z. Horita, Mater. Sci. Eng. A 503 (2009) 32–36.
[23] X.G. Qiao, M.J. Starink, N. Gao, Mater. Sci. Eng. A 513–514 (2009) 52–58.
[24] R.K. Roy, S. Das, J. Mater. Sci. 41 (2006) 289–292.
[25] T. Ungár, Adv. Eng. Mater. 5 (2003) 323–329.
[26] A. Dubravina, M.J. Zehetbauer, E. Schafler, I.V. Alexandrov, Mater. Sci. Eng. A 387–389 (2004) 817–821.
[27] R.Z. Valiev, R.K. Islamgaliev, I.V. Alexandrov, Prog. Mater. Sci. 45 (2000) 103–189.
[28] C.Y. Yu, P.L. Sun, P.W. Kao, C.P. Chang, Mater. Sci. Eng. A 366 (2004) 310–317.
[29] W.Q. Cao, A. Godfrey, W. Liu, Q. Liu, Mater. Lett. 57 (2003) 3767–3774.
[30] E. Hosseini, M. Kazeminezhad, Comput. Mater. Sci. 50 (2011) 1123–1135.
[31] N. Tsuji, Y. Ito, Y. Saito, Y. Minamino, Scr. Mater. 47 (2002) 893–899.